Optical design of a hollow cube-corner retroreflector for a geosynchronous satellite

Atsushi Minato, Satoru Ozawa, and Nobuo Sugimoto

The optical characteristics of a single-element hollow cube-corner retroreflector for a geosynchronous satellite were numerically evaluated for laser ranging and laser long-path absorption measurements of atmospheric species. An optical design with spherical surfaces and tuned dihedral angles was considered to compensate for velocity aberrations. The parameters for the retroreflector were optimized with genetic algorithms for different retroreflector sizes and wavelengths (500 nm and 1, 3, and 10 μm). We found that 20-cm retroreflectors are sufficient for realistic measurements when the laser wavelength is 500 nm or 1 μm. However, a larger retroreflector is necessary to overcome the detector noise level at 3 and 10 μm. © 2001 Optical Society of America

OCIS codes: 280.1120, 280.3640, 080.2740.

1. Introduction

We conducted experiments on an Earth–satellite–Earth laser long-path absorption method by using the retroreflector in space (RIS) on the Advanced Earth Observation Satellite (ADEOS) that was launched in August 1996.[1–4] The RIS is a large, single-element, hollow cube-corner retroreflector instead of an array of retroreflectors, which avoids the interference of reflected light between array elements. Although operation of the ADEOS and the RIS was discontinued ten months after launch, we experimentally confirmed the performance of the RIS. A single-element space retroreflector is useful as a target for multicolor laser ranging that can be used to calibrate atmospheric dispersion and achieves highly accurate measurements.[5,6] Measurement opportunities of only a few minutes occurred only once a day for the RIS experiment, because the ADEOS is a Sun-synchronous, polar-orbiting satellite.

A retroreflector on a geosynchronous satellite has several advantages. One retroreflector covers a wide area over the Earth. Multiple ground laser transmitter–receiver systems can measure information simultaneously with regard to changes in the densities of trace species throughout the day by use of laser long-path absorption measurements. Moreover, we can construct a simpler ground laser transmitter–receiver system than one for lower-altitude satellites because it is easier to track a geosynchronous satellite.

However, the altitude of geosynchronous satellites is approximately 50 times higher than that of polar-orbit satellites. Consequently, the optical efficiency of the measurement is much lower. We must still consider velocity aberrations, because the tangential velocities differ between the ground and the satellite.

We developed a method for optimizing the design of a retroreflector that utilizes a genetic algorithm.[7] We applied this technique to the optimization of single-element retroreflectors for geosynchronous satellites. We considered an optical design with spherical surfaces and tuned dihedral angles to compensate for velocity aberrations. We optimized the parameters for the retroreflector by using a genetic algorithm for different retroreflector sizes (mirrors of 20, 35, and 50 cm) and different wavelengths (500 nm and 1, 3, and 10 μm). We also estimated the signal intensity for a realistic ground laser transmitter–receiver system and discussed the feasibility of the measurement.

2. Retroreflector on a Geosynchronous Satellite

Figure 1 illustrates the concept of the measurement taken with a retroreflector on a geosynchronous satellite. The retroreflector can be used for laser long-

A. Minato (minato@base.ibaraki.ac.jp) and S. Ozawa are with the Graduate School of Science and Engineering, Ibaraki University, 4-2-1 Nakanarusawa, Hitachi 316, Japan. N. Sugimoto is with the National Institute for Environmental Studies, 16-2 Onogawa, Tsukuba 305, Japan.

Received 25 February 2000; revised manuscript received 27 November 2000.

0003-6935/01/091459-05$15.00/0

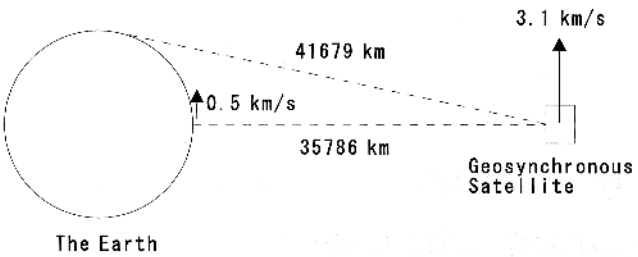

Fig. 1. Concept of measurements taken with a retroreflector on a geosynchronous satellite. Laser long-path absorption measurements and laser ranging with various zenith angles can be performed.

path absorption measurements and for lasers in the area shown in Fig. 1. The latitudinal and longitudinal angles from the satellite nadir are approximately 9 deg at the boundary.

The Lorentz transformation between the ground and the satellite gives the velocity aberration and the Doppler shift of reflected light. The tangential velocities of the geosynchronous satellite and the Earth's surface are 3.1 and 0.5 km/s. Therefore, the velocity aberration for the satellite nadir is approximately 17 μrad. The Doppler shift of 10-μm reflected light is 100 MHz at maximum.

Figure 2 shows an image of the retroreflector as observed from the ground. The aperture or diameter of the retroreflector is approximately 1.6 times the size of each side of each square mirror. When the laser wavelength is 1 μm and the aperture of the retroreflector is 50 cm, the divergence of the reflected beam that is due to Fraunhofer diffraction is approximately 5 μrad. Therefore, a retroreflector design similar to the RIS, with spherical surfaces and tuned dihedral angles, is required to receive the reflected laser beam efficiently on the ground.

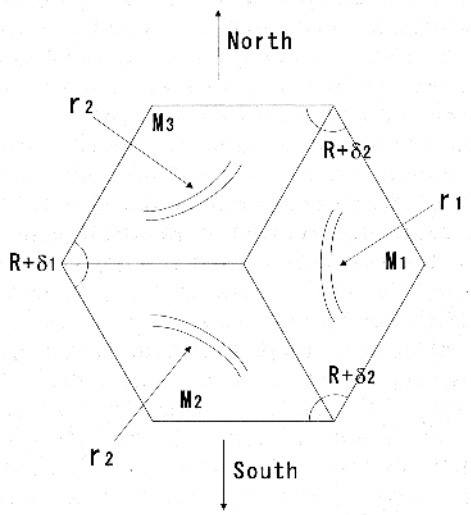

Fig. 2. Definition of the parameters of a single-element, hollow cube-corner retroreflector for a geosynchronous satellite. Two dihedral angles (δ_1 and δ_2) and two curvatures (r_1 and r_2) were optimized with the genetic algorithm.

3. Optimization of the Retroreflector with a Genetic Algorithm

We optimized single-element retroreflectors for a geosynchronous satellite. As shown in Fig. 2, we considered four parameters: two curvatures (r_1 and r_2) and two dihedral angles (δ_1 and δ_2). The optical axis of the retroreflector is directed to the nadir. δ_1 and δ_2 represent the right-angle differences. r_1 is the radius of curvature of convex mirror M_1, and r_2 is the radius of curvature of convex mirrors M_2 and M_3. We determined that the r_2 curvature of mirror M_2 is equal to the curvature of M_3, and the δ_1 dihedral angle between mirrors M_1 and M_2 is equal to the angle between mirrors M_1 and M_3. Our findings are based on the symmetry of satellite movement and the measurement configuration.

The optimization procedure by use of the genetic method is the same as that reported in Ref. 7. During optimization, four parameters, δ_1, δ_2, r_1 and r_2, are encoded in a gene that consists of arrays of 32 binary numbers, B_0 to B_{31}. In other words, one gene, or an array of B_0 to B_{31}, represents a set of dihedral angles and curvatures. δ_1 and δ_2 are represented by

$$\delta_1 = (B_0 + 2B_1 + 4B_2 + 8B_3 + 16B_4 + 32B_5 + 64B_6 + 128B_7) \times 0.66 \times 10^{-6}, \quad (1.1)$$

$$\delta_2 = (B_8 + 2B_9 + 4B_{10} + 8B_{11} + 16B_{12} + 32B_{13} + 64B_{14} + 128B_{15}) \times 0.66 \times 10^{-6}, \quad (1.2)$$

and r_1 and r_2 are represented by

$$1/r_1 = (B_{16} + 2B_{17} + 4B_{18} + 8B_{19} + 16B_{20} + 32B_{21} + 64B_{22} + 128B_{23}) \times 0.5 \times 10^{-6}, \quad (2.1)$$

$$1/r_2 = (B_{24} + 2B_{25} + 4B_{26} + 8B_{27} + 16B_{28} + 32B_{29} + 64B_{30} + 128B_{31}) \times 0.5 \times 10^{-6}. \quad (2.2)$$

When $1/r$ is zero, the mirror is flat. Each gene has a fitness value that determines the probability of selection in the genetic algorithm. The fitness values are determined as follows.

We considered five points on the ground, A–E, as shown in Fig. 3. We defined the fitness value as the minimum optical efficiency η for these five points. Point B represents a location at the satellite nadir. Points A, C, D, and E represent the locations at the boundary of the satellite coverage at which the measurement was taken. Optical efficiency η is defined by[3,7]

$$P_r = (16/\pi^2)(P_0/\theta_t^2)T^2\eta_{\mathrm{ret}}A_r\eta_{\mathrm{syst}}\eta, \quad (3)$$

where P_r is the received laser power, P_0 is the transmitted laser power, θ_t is the divergence of the transmitted laser beam, T is the atmospheric transmittance between ground and satellite, η_{ret} is the total reflectance of three mirrors, A_r is the aperture area of the receiver telescope, and η_{syst} is the optical efficiency of the receiver system. Optical ef-

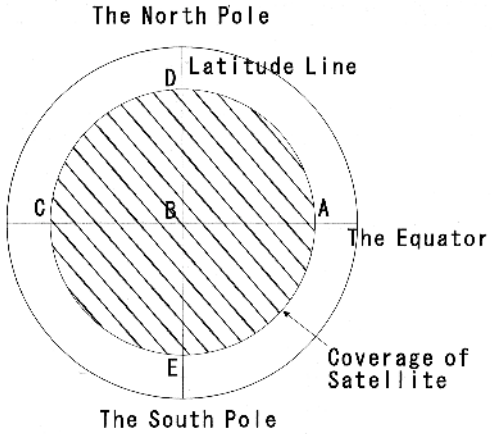

Fig. 3. Minimum optical efficiencies at five points on the ground, A–E, defined as fitness values.

ficiency η is in units of $[m^{-2}]$. The optical efficiency is the same for D and E because of symmetry.

By use of the genetic process,[8,9] including selection, crossover, and mutation, the best gene improves as the generations progress, which leads to the optimal design of a retroreflector.

4. Numerical Experiments and Discussion

We optimized the four parameters of the retroreflector for different retroreflector sizes and laser wavelengths by using the genetic algorithm. We considered three retroreflector sizes with mirrors of 20, 35, and 50 cm. We also considered four wavelengths: 10 μm for the CO_2 laser, 3 μm for the optical parametric oscillator, 1 μm for the YAG laser, and 500 nm for second-harmonic generation of a YAG laser. Many trace species are expected to be measured by Earth–satellite laser long-path absorption measurements in the 3–10-μm wavelength region.[10]

The genetic algorithm is the same as that reported in our previous paper.[7] We prepared 50 genes for one generation. We set the mutation probability at 5 bits/gene. A set of optimized designs was obtained for all cases, and fitness of the best genes was saturated for approximately the 50th generation. Table 1 lists these optimization parameters and their fitness, that is, the minimum of optical efficiencies. The optical efficiency is low when the size is small or the wavelength is long as a result of diffraction of the reflected beam.

Figure 4 shows examples of the optical efficiency distribution of optimized retroreflectors, indicating that the optimized fitness equals the minimum optical efficiencies in the coverage area on Earth. We evaluated the received signal on the ground. We used optimized fitness as the optical efficiencies, and the results are listed in Table 2. We focused on the realistic parameters of the laser transmitter–receiver system. For all the cases the parameters were 100-mJ transmitted laser power, 0.5 atmospheric transmittance, 0.9 total reflectance of three mirrors, a 1.5-m diameter ($A_r = 1.77\ m^2$) of the receiver telescope, and 0.1 optical efficiency of the receiver system.

The divergence of the transmitted laser beam was

Table 1. Optimized Parameters and Optical Efficiencies

Wavelength (μm)	Size (cm)	δ_1 (rad)	δ_2 (rad)	$1/r_1$ (m^{-1})	$1/r_2$ (m^{-1})	η
0.5	20	0.0	1.0×10^{-5}	3.0×10^{-7}	3.0×10^{-7}	2.2×10^{-22}
0.5	35	0.0	8.0×10^{-6}	0.0	3.0×10^{-7}	1.3×10^{-21}
0.5	50	0.0	1.0×10^{-7}	1.0×10^{-7}	3.0×10^{-6}	1.7×10^{-21}
1.0	20	0.0	1.0×10^{-5}	6.0×10^{-7}	0.0	5.8×10^{-23}
1.0	35	0.0	1.0×10^{-5}	1.0×10^{-7}	1.0×10^{-7}	5.6×10^{-22}
1.0	50	0.0	9.8×10^{-6}	0.0	1.0×10^{-7}	2.1×10^{-21}
3.0	20	0.0	9.8×10^{-6}	1.0×10^{-5}	7.0×10^{-7}	6.9×10^{-24}
3.0	35	0.0	1.1×10^{-5}	0.0	7.0×10^{-7}	5.5×10^{-23}
3.0	50	0.0	1.1×10^{-5}	0.0	0.0	2.7×10^{-22}
10.0	20	3.3×10	1.7×10^{-7}	3.0×10^{-7}	0.0	3.1×10^{-24}
10.0	35	0.0	4.3×10^{-6}	0.0	2.5×10^{-5}	1.1×10^{-23}
10.0	50	3.3×10^{-7}	6.7×10^{-7}	0.0	2.4×10^{-5}	2.9×10^{-23}

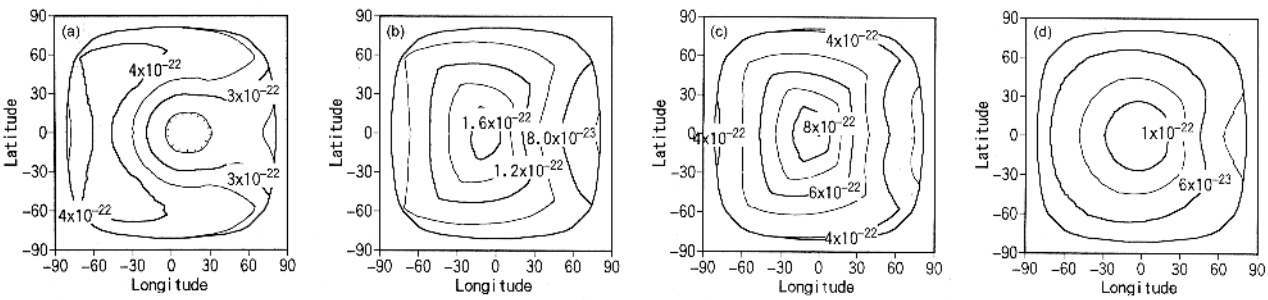

Fig. 4. Examples of the optical efficiency distribution of optimized retroreflectors: (a) 20-cm mirror, 500 nm; (b) 20-cm mirror, 1 μm; (c) 50-cm mirror, 3 μm; (d) 50-cm mirror, 10 μm.

Table 2. Parameters Used to Estimate the Received Signals and the Results

	Wavelengths			
	500 nm[a]	1 μm[a]	3 μm[b]	10 μm[b]
η (m^{-2})	2.2×10^{-22}	5.8×10^{-23}	2.7×10^{-22}	2.9×10^{-23}
P_0 (J)	0.1	0.1	0.1	0.1
θ_t (rad)	1.0×10^{-4}	8.7×10^{-5}	7.0×10^{-5}	5.5×10^{-5}
T	0.5	0.5	0.5	0.5
η_{ret}	0.9	0.9	0.9	0.9
η_{syst}	0.1	0.1	0.1	0.1
A_r (m^2)	1.77	1.77	1.77	1.77
D^* (cm $Hz^{1/2}$ W^{-1})	—	—	6×10^{10}	1×10^{10}
A_d (cm^2)	—	—	1×10^{-4}	1×10^{-4}
τ (s)	—	—	1×10^{-7}	1×10^{-7}
P_r (Photoelectrons)	350	250	5400	3100
N_d (Photoelectrons)	—	—	800	2300

[a]20-cm mirror.
[b]50-cm mirror.

determined from the coherent length of the atmosphere.[11] When the atmospheric turbulence is small, the coherent length of the atmosphere is approximately 10 cm at 500 nm. The coherent length, $\rho(\lambda)$, depends on the wavelength and the zenith angle, as

$$\rho(\lambda) = \rho(\lambda_0)\,(\lambda/\lambda_0)^{1.2}\,(\cos Z)^{0.6}, \tag{4}$$

where λ is the wavelength, λ_0 is 500 nm, and Z is the zenith angle. The diffraction from an aperture, that is, 10-cm coherent length, is 12 μrad at 500 nm when the zenith angle is 0 deg. To estimate the received signal, we used a beam divergence value of 0.1 mrad, which is eight times larger than the diffraction from a 10-cm aperture at 500 nm, which was also a reasonable value for the RIS experiment. We determined the beam divergence at other wavelengths by considering the wavelength dependence of the coherent length.

We estimated the received laser power with Eq. (3) and by using the parameters in Table 2. When the laser wavelength is 500 nm and the length of the mirror is 20 cm, the received signal is 350 photoelectrons; when the laser wavelength is 1 μm and one side of the mirror is 20 cm, the received signal is 250 photoelectrons. The optimized designs of 20-cm retroreflectors for 500 nm and 1 μm are sufficient for realistic laser-ranging measurements.

The detector noise is dominant in the infrared region. The detector noise-equivalent photoelectron number N_d is written as

$$N_d = (A_d\tau)^{1/2}/(D^* h\nu), \tag{5}$$

where A_d is the area of the detector, τ is the time constant of photodetection, D^* is the detectivity, and $h\nu$ is the energy of a single photon.

If the laser wavelength is 3 μm and the mirror is 50 cm, the received signal is 5400 photoelectrons. At 10 μm, if the mirror were 50 cm, the received signal would be 3100 photoelectrons. These expected signals are larger than the estimated detector noises listed in Table 2.

The detectivity can be improved by reduction of the detector field of view and by use of a cold filter to reduce the background radiation. A higher signal-to-noise ratio can be achieved when heterodyne detection is employed.

5. Conclusion

We numerically evaluated the optical efficiency of a single-element retroreflector on a geosynchronous satellite as a target of laser long-path absorption measurements and laser ranging. First, we performed optimization on the designs of retroreflectors of various sizes and wavelengths by use of the genetic algorithm. We then evaluated the received signal, taking into consideration the realistic parameters of the ground system. We found that 20-cm retroreflectors are sufficient for realistic measurements when the laser wavelength is 500 nm or 1 μm. However, a larger retroreflector, such as 50 cm, is necessary to overcome the detector noise level at 3 and 10 μm.

References

1. A. Minato, N. Sugimoto, and Y. Sasano, "Optical design of cube corner retroreflectors having curved mirror surfaces," Appl. Opt. **31,** 6015–6020 (1992).
2. N. Sugimoto and A. Minato, "Data reduction method for the laser long-path absorption measurement of atmospheric trace species using the retroreflector in space," IEICE Trans. Commun. **E78-B,** 1585–1590 (1995).
3. N. Sugimoto and A. Minato, "Optical characteristics of the Retroreflector in Space for the Earth Observing Satellite," Opt. Rev. **3,** 62–64 (1996).
4. N. Sugimoto, N. Koga, I. Matsui, Y. Sasano, A. Minato, K. Ozawa, Y. Saito, A. Nomura, T. Aoki, T. Itabe, H. Kunimori, I. Murata, and H. Fukunishi, "Earth–satellite–Earth laser long-path absorption experiment using the Retroreflector in Space (RIS) on the advanced earth observing satellite," J. Opt. A: Pure Appl. Opt. **1,** 201–209 (1999).
5. S. Riepl, U. Schreiber, and W. Schlueter, "WLRS streak camera experiment," in *Laser Radar Ranging and Atmospheric Lidar Techniques*, U. Schreiber and C. Werner, eds., Proc. SPIE **3218,** 19–30 (1997).
6. T. W. Zagwodzki, J. F. McGarry, J. J. Degnan, and T. K.

Varghese, "Two-color SLR experiments at the GSFC 1.2-m telescope," in *Laser Radar Ranging and Atmospheric Lidar Techniques*, U. Schreiber and C. Werner, eds., Proc. SPIE **3218,** 113–124 (1997).
7. A. Minato and N. Sugimoto, "Design of four-element, hollow-cube corner retroreflector for satellites by use of a genetic algorithm," Appl. Opt. **37,** 438–442 (1998).
8. J. H. Holland, *Adaptation in Natural and Artificial Systems* (MIT, Cambridge, Mass., 1992).
9. D. E. Goldberg, *Genetic Algorithms in Search, Optimization, and Machine Learning* (Addison-Wesley, Reading, Mass., 1989).
10. N. Sugimoto, A. Minato, K. Ozawa, Y. Saito, and A. Nomura, "Theoretical evaluation of Earth-to-satellite laser long-path absorption measurement of atmospheric trace species in the infrared region," Jpn. J. Appl. Phys. **34,** 2329–2334 (1995).
11. G. Walker, *Astronomical Observations: an Optical Perspective* (Cambridge University, Cambridge, England, 1987).